Nanoscale

REVIEW

View Article Online
View Journal | View Issue

Cite this: *Nanoscale*, 2024, **16**, 16313

Carbon materials and their metal composites for biomedical applications: A short review

Su-Bin Kim, Choong-Hee Kim, Seul-Yi Lee* and Soo-Jin Park *

Carbon materials and their hybrid metal composites have garnered significant attention in biomedical applications due to their exceptional biocompatibility. This biocompatibility arises from their inherent chemical stability and low toxicity within biological systems. This review offers a comprehensive overview of carbon nanomaterials and their metal composites, emphasizing their biocompatibility-focused applications, including drug delivery, bioimaging, biosensing, and tissue engineering. The paper outlines advancements in surface modifications, coatings, and functionalization techniques designed to enhance the biocompatibility of carbon materials, ensuring minimal adverse effects in biological systems. A comprehensive investigation into hybrid composites integrating carbon nanomaterials is conducted, categorizing them as fullerenes, carbon quantum dots, carbon nanotubes, carbon nanofibers, graphene, and diamond-like carbon. The concluding section addresses regulatory considerations and challenges associated with integrating carbon materials into medical devices. This review culminates by providing insights into current achievements, challenges, and future directions, underscoring the pivotal role of carbon nanomaterials and their metal composites in advancing biocompatible applications.

Received 14th May 2024,
Accepted 30th July 2024

DOI: 10.1039/d4nr02059f

rsc.li/nanoscale

1. Introduction

The medical device industry has rapidly expanded globally, propelled by an increasing prevalence of accidental injuries, vehicle accidents, diseases, and related fatalities. This growth underscores the integral role that medical devices play in healthcare systems.[1–3] According to the World Health Organization (WHO), more than 2 million distinct medical devices are used worldwide, encompassing equipment, machinery, implants, software, and materials.[4–6] The global biomedical applications market is projected to reach USD$32 billion by 2031, experiencing a compound annual growth rate of 11%.[7]

Various materials have been commercialized for medical applications, including stainless steel and titanium for implants, polymers such as polyethylene and polypropylene for prosthetics, and ceramics like alumina and zirconia for specific orthopedic uses. These advancements aim to save millions of lives and extend life expectancy.[8–10] However, these materials still have certain limitations arising from the inherent properties of materials. Metals can corrode and wear over time, risking implant failure. Polymers may degrade mechanically and have limited biocompatibility. Ceramics can be brittle and fracture under stress. These issues underscore the need for advanced materials with enhanced performance and longevity in biomedical applications.[11–13]

Biocompatibility remains a cornerstone in both the medical and biomaterials fields, revolving around a material's ability to interact seamlessly with biological systems, particularly when in contact with living tissue or organisms.[14–17] This fundamental consideration is crucial for ensuring the safety and efficacy of materials used in diverse biological environments.

A thorough evaluation of biocompatibility encompasses assessing factors such as non-toxicity, minimal inflammatory response, absence of allergenicity, and appropriate mechanical properties.[18–20] The primary objective is to achieve the safe integration of materials into biological systems, thus ensuring their effectiveness. However, issues related to processability, morphological stability, and chemical stability can lead to adverse reactions.[21–23] Overcoming these challenges requires a detailed approach that includes material selection, design, testing, and development across various research phases.

Carbonaceous nanomaterials are becoming increasingly valuable in biomedical applications owing to their inherent biocompatibility, making them ideal candidates for drug delivery, bioimaging, and biosensing.[24–26] Their unique characteristics, such as extensive surface area and high electrical conductivity, also enable versatile functions in diagnostics, therapeutics, tissue engineering. These materials are particularly beneficial in applications such as neural interfaces and biosensors, where their lower tendency to provoke immune

Department of Chemistry, Inha University, Incheon 22212, Republic of Korea.
E-mail: sjpark@inha.ac.kr, leesy1019@inha.ac.kr

responses is crucial for long-term biological interactions, especially in implantable organ devices.

The adaptability of carbon materials is further enhanced by their ability to be modified with diverse functional groups and biomolecules, which improves their interactions with biological systems.[27–32] This flexibility allows for the customization of surface properties to interact with living organisms and elicit specific cellular responses. Carbonaceous nanomaterials, available in various forms like particles, tubes, aerogels, and thin films, can be tailored for specific biomedical applications, ranging from drug delivery carriers to tissue engineering scaffolds.[33,34]

The structural diversity of carbonaceous nanomaterials, including zero-dimensional (0D) to three-dimensional (3D), possess unique properties that make them suitable for various medical applications. Carbon quantum dots (CQDs), with their 0D nanoscale particle structure, exhibit unique optical (visible to Ultra-violet) and electronic properties for use in drug delivery, bioimaging, and sensing.[35,36] Carbon nanotubes (CNTs), which are 1D cylindrical formations from rolled graphene sheets, exhibit excellent mechanical strength (Young's modulus up to 320–1470 GPa for Single-walled CNTs) and electrical conductivity (10^3–10^5 S m^{-1}), with potential applications as drug carriers, imaging agents, and tissue engineering scaffolds.[37,38] Carbon nanofibers (CNFs) are composed of sp^2-based 1D filaments arranged in a crystalline formation, exhibit high mechanical strength and lightweight properties with exceptional tensile strength (2–3 GPa), making them stronger than steel while being significantly lighter.[39,40] Graphene, characterized by its two-dimensional (2D) hexagonal lattice of carbon atoms, is noted for its superior mechanical (Young's modulus up to 1000 GPa), thermal (~5000 W m^{-1} K^{-1}), and electrical properties (~10^6 S m^{-1}), and explored for applications such as drug delivery, biosensors, and imaging due to its large surface area and ease of functionalization.[41,42] Diamond-like carbon (DLC), a 3D carbon material with a structure similar to diamond, is known for its exceptional hardness, biocompatibility, and wear resistance, leading to applications in medical coatings, implants, and protective coatings.[43,44]

Despite the excellent properties of carbon materials, their long-term biocompatibility in biomedical applications can be problematic due to potential cytotoxicity and inflammatory responses. Additionally, the variability in the purity and consistency of carbon materials can lead to unpredictable biological interactions. To overcome these biocompatibility issues, rigorous purification processes can be implemented to ensure the consistency and quality of carbon materials. Surface functionalization with biocompatible coatings can reduce cytotoxicity and minimize inflammatory responses.[45,46]

Over the past two decades, extensive research has been conducted to enhance the physicochemical properties of carbonaceous materials through various functionalization strategies, such as heteroatom doping or metal coating.[47,48] These studies primarily focus on hybrid composites that incorporate heteroatoms such as nitrogen (N), sulfur (S), phosphorus (P), boron (B), and fluorine (F), as well as metals like zinc (Zn), magnesium (Mg), gold (Au), silver (Ag), copper (Cu), and gallium (Ga). Particular emphasis is placed on metals such as Ag, Au, and Ga due to their lower toxicity and environmental friendliness compared to other metals.[49,50] These studies aim to improve key properties such as biocompatibility, antimicrobial activity, mechanical strength, and electrical conductivity. The development of these hybrid composites is expected to drive innovation in the biomedical field, leading to more effective and safer therapeutic approaches.

Despite numerous reviews on metal-doped carbon materials, a comprehensive analysis of the advantages of different types of carbon materials for functionalization in the biomedical field remains lacking. This gap highlights the need for a thorough examination of the benefits of various carbon materials and their hybrid metal composites in biomedical applications.

This review aims to explore various strategies for enhancing the biocompatibility of carbon nanomaterials, with a focus on surface functionalization and hybridization with metals for nanocomposites. It emphasizes recent advancements in carbonaceous materials and their metal composites for biomedical applications, categorized by their dimensions; fullerenes, CQD, CNT, CNFs, graphene, and DLC. By providing insights into improving the seamless integration of carbon nanomaterials in biomedical applications, this review seeks to highlight their potential to drive innovation in medical technologies and therapies. Fig. 1 illustrates the main components discussed in this study of carbon nanomaterials and their relevance to biocompatibility in the human body.

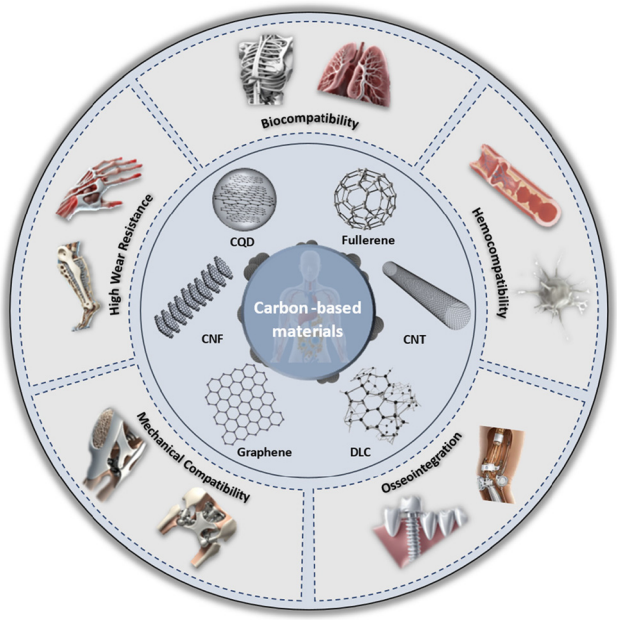

Fig. 1 Biomedical characteristics and applications of carbonaceous nanomaterials and their hybrid composites discussed in this review.

2. Carbon materials and their metal composites for biomedical applications

Fig. 2 illustrates the number of publications in the biomedical field focusing on carbon-based materials, metal-based materials, and their hybrid carbon/metal composites over the past decade. It highlights a significant upward trend, reflecting the growing interest and expanding research efforts in utilizing these materials for various biomedical applications. The increase in publications suggests advancements in understanding the unique properties of carbon-based materials as well as metals, such as their biocompatibility, mechanical strength, and functional versatility. This rising trajectory also indicates a broader acceptance and recognition of carbon-based materials in developing innovative solutions for medical devices, drug delivery systems, tissue engineering, and other therapeutic areas.

This section reviews the various applications of different types of carbonaceous materials and their metal composites, detailing strategies such as metal doping, surface treatment, and functionalization used to enhance these materials. Emphasis is placed on the unique properties of carbon-based nanomaterials, both individually and in combination with metals, highlighting their contributions to a wide range of various biomedical applications.

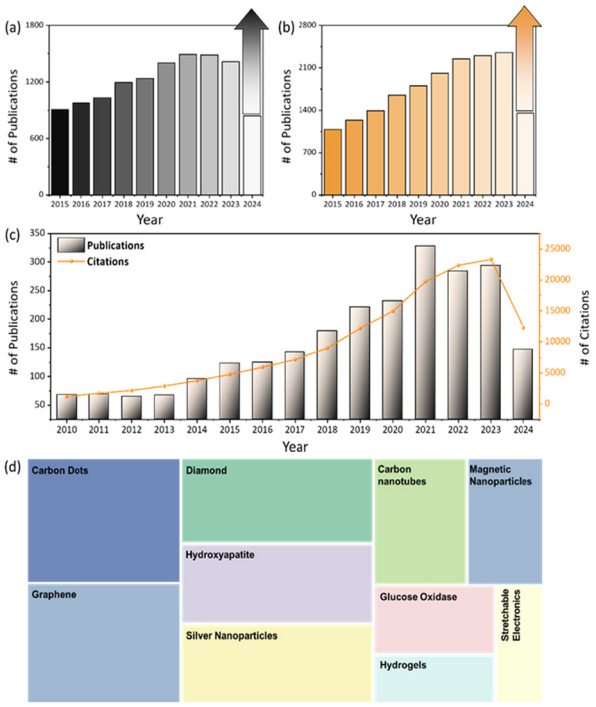

Fig. 2 (a) Number of publications in the biomedical field based on carbon-based materials and (b) number of publications in the biomedical field based on metal-based materials; (c) number of publications and citations in the biomedical field with carbon materials and their metal composites; (d) the most widely used carbon-based materials in the biomedical field. (All publication and citation data were from the Web of Science, 2010–2024).

2.1. Fullerenes and their metal composites

Fullerenes are a class of carbon allotropes in which carbon atoms are bonded together to form a spherical structure of varying widths. They are composed entirely of carbon, taking the form of a cage-like fused-ring structure consisting of hexagons and pentagons, offering attractive optical, electrochemical, and physical properties for various medical fields, such as drug delivery to specific target cells or tissues.[51] Their insolubility in nature has increased interest in biological applications.[52] Fullerenes possess chemically and structurally stable structures, making them suitable for photodynamic therapy. They act as targeted vectors for mineralized bone and photosensitizers, effectively generating reactive oxygen species with specific wavelengths of light to selectively destroy cancer cells.[53–55] For instance, C_{60} has been characterized as an human immunodeficiency virus (HIV) inhibitor,[56] magnetic resonance imaging (MRI) contrast agent,[57] antioxidant,[58] and antibacterial agent.[59]

Anusha *et al.* developed an electrochemical sensor using a C60 and bimetallic (Cu–Ni) nanoparticle (NPs) nanocomposite film-modified glassy carbon electrode (GCE) to enhance the oxidation of vitamin D_3 and measure its concentration in blood samples.[60] The sensor was fabricated by drop-casting C_{60} onto the GCE, followed by electrochemical deposition of CuNPs and NiNPs onto the fullerene-modified GCE (Fig. 3a). The resulting sample showed a well-defined oxidation peak for detecting vitamin D_3, with a dynamic concentration range of 1.25–475 μM and a detection limit of 0.0025 μM (Fig. 3b). The platform demonstrated superior analytical performance with a low detection limit, a wide working range, high sensitivity, excellent reproducibility, and stability.

Endohedral metallofullerenes (EMFs) are exceptional carriers for rare earth element (REE) ions in biomedical applications due to their ability to prevent the release of toxic metal ions.[61] A study introduced the concept of metallobuckytrio (MBT), a threebuckyball system, as a platform to develop structurally defined water-soluble EMF derivatives with customizable polymer ligands, ensuring superb biocompatibility.[62] The safety of water-soluble MBTs is confirmed by inductively coupled plasma mass spectrometry (ICP-MS) to verify the EMF cage confinement of metal ions, and cytotoxicity studies on different cell lines, where MBTs were found to be generally non-toxic (Fig. 3(c and d)). The Lu MBTs, a type of MBT, demonstrate superior T_1 relaxivity compared to typical Gd complexes, potentially surpassing current clinical MRI contrast agents in safety and efficiency. Additionally, Lu MBTs generate reactive oxygen species upon light irradiation, showing promise as photosensitizers in biomedical applications.

The EMF and trimetallic nitride endohedral fullerenes (TNT-EMF) have been also recognized for their multifunctional capabilities, particularly in combating oxidative stress and inflammation. Li *et al.* developed carboxyl-$Gd_3N@C_{80}$, a specific type of functionalized fullerene, which exhibits robust

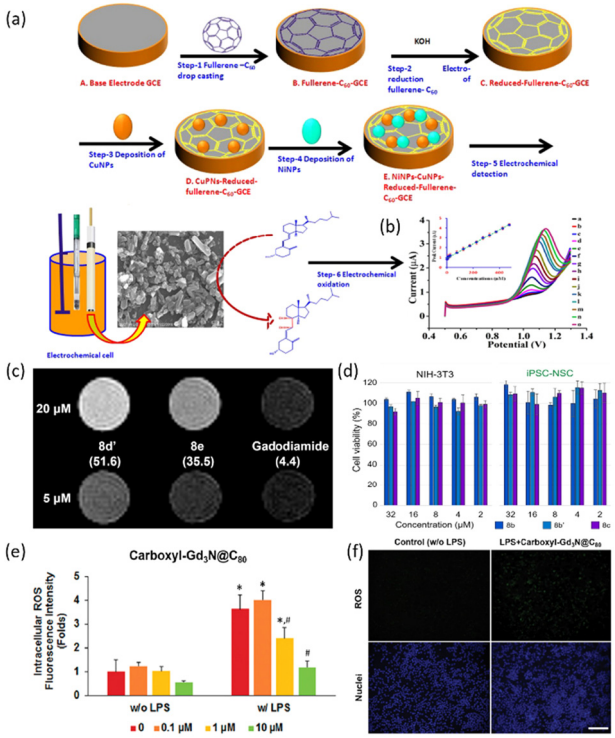

Fig. 3 (a) Illustration of electrochemical sensor fabrication procedure for Cu–Ni NPs@C_{60} nanocomposite film; (b) nanocomposite at CuNPs-NiNPs@reduced-fullerene-C_{60}/GCE with different concentrations of vitamin D_3: 1.25, 2.5, 5, 10, 20, 25, 75, 125, 175, 225, 275, 325, 375, 425 and 475 μM (a–o) (inset: calibration plot between peak current and vitamin D_3 concentration). Reproduced with permission from ref. 60 Copyright © 2020 Elsevier; (c) MR imaging of Gd MBT solutions on a 1.0 T scanner. The measured r_1 values at 1.4 T are written in parentheses under each compound, in the unit of mM^{-1} s^{-1}; (d) cell viability tests of MBTs 8b, 8b′ and 8c at concentrations of 2–32 μM against NIH-3T3 and iPSC-NSC cell lines (error bars indicate standard deviation of individual cell viability data set) Reproduced with permission from ref. 62 Copyright © 2022 WILEY-VCH Verlag GmbH & Co. (e) Carboxyl-Gd3N@C_{80} dose-dependently attenuates LPS-induced excess ROS; (f) representative fluorescence images of intracellular ROS illustrated robust ROS-scavenging activity of carboxyl-Gd_3NC_{80}. Image taken at ×200 magnification. Scale bar represented 100 μm. *p < 0.05 *vs.* non-LPS control, #p < 0.05 *vs.* LPS-treated groups. Reproduced with permission from ref. 63 Copyright © 2017 ACS.

radical scavenging properties and can suppress lipopolysaccharide (LPS)-induced reactive oxygen species (ROS) in macrophages, indicating its potential in combating oxidative stress (Fig. 3(e and f)).[63] The sample has also demonstrated anti-inflammatory effects by attenuating the expression of pro-inflammatory markers like iNOS and TNF-α, while increasing the expression of antioxidative enzymes like HO^{-1} and Nrf2, possibly through ERK signaling pathways. These results have shown that fullerenes act as powerful antioxidants due to their ability to react with free radicals, making them effective in various biomedical applications. Further, encapsulating metal nanoparticles within the fullerene structure merges the structural stability of fullerenes with the functional properties of metals. This approach protects the metal nanoparticles, leveraging their long-term stability and efficient drug delivery *in vivo*, thereby maximizing therapeutic efficacy.

2.2. CQDs and their metal composites

Carbon quantum dots (CQDs) have garnered significant attention in the biomedical field due to their high sensitivity to local environmental changes.[64–66] While traditional quantum dots (QDs) are known for their stable fluorescence, their high toxicity due to heavy metal content makes them less desirable.[67,68] CQDs, on the other hand, present a promising alternative, offering high biocompatibility, cost-effectiveness, and chemical inertness, making them suitable for clinical fluorescent applications. The strong and tunable fluorescence properties of CQDs make them vital imaging agents for live cell imaging and monitoring cellular processes.[69,70] Furthermore, CQDs exhibit photothermal conversion properties, where absorbed light is converted into thermal energy. This characteristic is strategically utilized in photothermal therapy, enabling controlled heat release upon laser irradiation to selectively target cancer cells.

Nafchi *et al.* synthesized hybrid nanocomposites of Fe_3O_4 nanoparticles doped with glutaric acid-functionalized CQDs.[69] The Fe_3O_4/CQD nanocomposites exhibited high efficiency in doxorubicin (DOX) loading, effectively attaching the positively charged DOX to the negatively charged Fe_3O_4/CQDs through an electrostatic absorption mechanism. The loading efficiency and capacity of Fe_3O_4/CQD were determined to be 94% and 37.2 mg DOX g^{-1} of magnetic nanoparticles (MNPs), respectively. Fluorescence imaging confirmed the ability of Fe_3O_4/CQD to target MCF-7 and HFF cells, as shown in Fig. 4(a), and T_2-weighted magnetic resonance imaging (MRI) scans of Fe_3O_4/CQD in aqueous solution showed a high r_2 relaxivity (86.6 mM^{-1} s^{-1}). These results indicate that this nanocomposite is a promising candidate for highly efficient T_2 contrast agents in MRI. Furthermore, MTT cell viability assays revealed that DOX-loaded Fe_3O_4/CQD exhibited high biocompatibility with HFF cells (95% viability) and significant cytotoxicity towards MCF-7 cancer cells (45% viability) (Fig. 4(b)). This demonstrated the efficacy and selectivity of the drug delivery system, highlighting the potential of Fe_3O_4/CQD for targeted diagnosis and therapy. As a result, the synthesized Fe_3O_4/CQD nanocomposite possesses superparamagnetic and fluorescent properties suitable for medical applications such as MRI, targeted drug delivery, and cancer cell labelling and tracking.

Sarkar *et al.* prepared Fe_3O_4 NPs-doped CQD (CQD@Fe_3O_4) using a wet chemical co-precipitation method.[71] Cytotoxicity assays on RAW 264.7 cells at various concentrations (15.6, 31.5, 62.5, 125, and 250 μg m^{-1}) demonstrated significantly improved biocompatibility of CQD@Fe_3O_4 compared to bare Fe_3O_4, as shown in Fig. 4(c). In detail, at 250 μg ml^{-1}, Fe_3O_4 maintained only 69% cell viability, whereas CQD@Fe_3O_4 exhibited an enhanced cell viability of 87%. At lower concentrations (15.6 and 31.5 μg ml^{-1}), bare Fe_3O_4 and CQD@Fe_3O_4 showed cell viability of 84 and 96%, respectively. Side scattering cell (SSC) uptake studies revealed that cell granularity

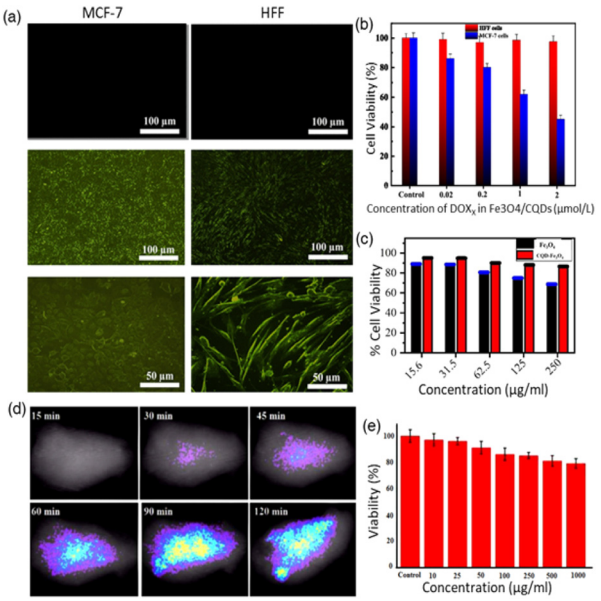

Fig. 4 (a) Fluorescence microscopy images of MCF-7 cancer cells (left) and normal HFF cells (right), both untreated and treated with Fe_3O_4/CQDs at 100 μm and 50 μm (excitation at 488 nm), alongside results from the MTT assay; (b) viability of HFF and MCF-7 cells in contact with DOX-loaded Fe_3O_4/CQD nanocomposites at different drug concentrations for 24 h, both with and without an applied magnetic field. Statistical significance indicated by $*p < 0.05$ and $**p < 0.01$ compared to control. Reproduced with permission from ref. 69 Copyright © 2022 ACS. (c) Cytotoxicity assay for Fe_3O_4 NPs and CQD@Fe_3O_4 NPs at concentrations ranging from 15.6 μg ml^{-1} to 250 μg ml^{-1}. Reproduced with permission from ref. 71 Copyright © 2020 IOP science. (d) *In vivo* fluorescence imaging of Mn/CQD/SiO_2@naproxen. (e) MTT assay: HEK-293 cell treatment with Mn/CQD/SiO_2@naproxen for 24 h. Reproduced with permission from ref. 72 Copyright © 2021 Elsevier.

remained unchanged even at a significantly high CQD concentration of 1600 μg ml^{-1}, indicating that CQD@Fe_3O_4 did not adversely affect cell morphology. Vitamin D_2 detection using differential pulse voltammetry also achieved a sensitivity of 0.069 μA ng^{-1} ml cm^{-2} and a detection limit of 2.46 ng ml^{-1}, demonstrating the potential of CQDs for sensitive and selective electrochemical biosensing.

Ardestani *et al.* developed a biocompatible nano-carrier of Mn/CQD/SiO_2, which integrates magnetic carbon quantum dots (CQDs) modified with mesoporous silica for enhanced drug delivery and tracking (Fig. 4(d and e)).[72] The silica modification improved biocompatibility and minimized cytotoxicity. The conjugation of naproxen to the nanoprobe, forming Mn/CQD/SiO_2@naproxen, allowed for detailed biodistribution studies. The fluorescence imaging provided insight into the biodistribution of naproxen, which was corroborated by COX gene expression levels indicating increased accumulation in the liver and decreased COX production (Fig. 4d). In addition, MTT assays on HEK-293 cells indicated no adverse effects from Mn/CQD/SiO_2@naproxen (Fig. 4e). These results highlight the unique properties of Mn/CQD/SiO_2, including excellent biocompatibility, minimal toxicity, and magnetic and fluorescent properties, underscoring the pivotal role of CQDs in enhancing the nanocarrier's potential for biomedical applications.

Overall, CQDs offer significant advantages in biomedical applications due to their exceptional reducing capabilities, making them highly effective for generating metal-doped carbon dots *in situ*.[73,74] These CQDs serve as both reducing agents and stabilizers for metal nanoparticles, and their integration with magnetic nanoparticles enables the creation of multimodal imaging platforms that combine optical and magnetic resonance imaging. CQDs are effective in multimodal, image-guided, near-infrared-responsive chemo-phototherapy, and exhibit superior properties in enhanced antimicrobial activity and the development of advanced imaging and therapeutic platforms.[75,76] Their ability to generate light-induced reactive oxygen species (ROS) is enhanced by upconversion photoluminescence and efficient photon-induced electron transfer, improving their photocatalytic antibacterial properties. These properties contribute to preventing the recombination of photo-induced electron–hole pairs, thereby enhancing the photocatalytic antibacterial properties of CQDs.[77]

2.3. CNTs and their metal composites

CNTs have emerged as a versatile and promising material in biomedical applications due to their unique structural, mechanical, and electrical properties. In particular, extensive research is highlighting the potential of CNTs, emphasizing their ability to improve functionality and durability in orthopedic applications. Additionally, the biocompatibility of CNTs makes them a promising biomaterial for various medical and healthcare applications, facilitating the improvement of prosthetic devices and the development of functional matrices for targeted anatomical treatments. Their versatility, manifested in forms such as films, fibers and 3D structure, allows for adaptable biomaterial design tailored to specific medical needs. In addition, their tubular structure allows encapsulation of drugs, facilitating controlled and targeted release in medical treatments.

Abazari *et al.* synthesized magnesium oxide (MgO) NPs-loaded CNTs for the reinforcement of Mg–3Zn–1Mn alloy (ZM31 alloy) using a semi-powder metallurgy approach, followed by hot extrusion.[78] The MTT assay revealed higher cell viability in ZM31/CNTs and ZM31/MgO-CNTs composite extracts compared to Mg alloy extracts, with increased cell activity over time (Fig. 5(a)). This indicates that CNTs significantly enhance the biocompatibility of Mg-based composites. CNTs stimulate cell functions by adsorbing proteins with specific characteristics, thereby promoting cell growth. The improved cellular compatibility of the ZM31/CNTs composite is attributed to the rough nano-scaled surface topography provided by CNTs. ALP staining demonstrated that MG-63 cells cultured on ZM31/MgO-CNTs composites exhibited more intense ALP activity, indicating enhanced early cell differentiation compared to those on Mg alloy and ZM31/CNTs composites (Fig. 5(b)). Fluorescence imaging confirmed normal osteoblast growth on all composites, with a significant increase in cell population on ZM31/MgO-CNTs (Fig. 5(c)).

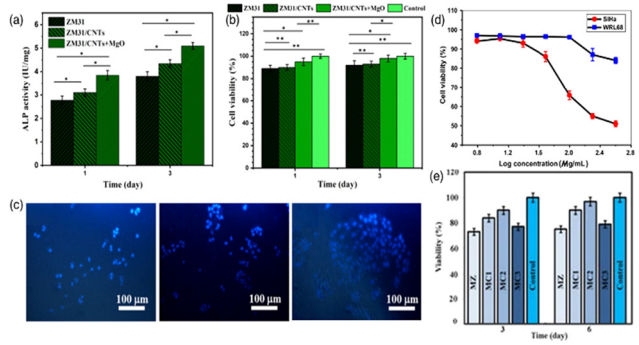

Fig. 5 (a) Cell viability and (b) ALP activity of MG-63 cells cultured for various durations on ZM31 alloys, ZM31/CNTs, and MgO-ZM31/CNTs nanocomposites, (c) MG-6 cells and fluorescent DAPI staining of these cells grown on: ZM31 alloy, ZM31/CNTs, and ZM31/MgO-CNTs nanocomposites for 3 days (*p < 0.05 and **p < 0.01). Reproduced with permission from ref. 78 Copyright © 2022 Elsevier. (d) MTT cell viability assay results for SiHa and WRL68 cells incubated with SWNTs–TiO2/Ag. Reproduced with permission from ref. 79 Copyright © 2019 Springer. (e) Cell viability of MG63 cells cultured over varying durations on MZ, MC1, MC2, and MC3 biocomposites. Reproduced with permission from ref. 80 Copyright © 2022 MDPI.

This improved cell response is due to the lower corrosion rate, slower ion release, and maintained pH balance. These findings highlight the critical role of CNTs in enhancing the biocompatibility and cell attachment of Mg-based composites.

Ahmed *et al.* synthesized conjugates comprising single-wall nanotubes (SWNTs) and multi-wall nanotubes (MWNTs) integrated with silver-doped titanium dioxide (TiO_2/Ag), exhibiting antimicrobial and cytotoxic properties.[79] The study commenced with the chemical treatment of crude SWNTs and MWNTs using sulphuric acid and nitric acid, resulting in functionalized SWNTs (F-SWNTs) and MWNTs (F-MWNTs) surfaces. TiO_2/Ag NPs were then loaded onto these functionalized surfaces using an *in situ* sol–gel technique. Dispersion studies indicated that untreated SWNTs (R-SWNTs) and MWNTs (R-MWNTs) exhibited limited bactericidal activity against *Escherichia coli* (*E. coli*) and *Staphylococcus aureus* (*S. aureus*). In contrast, SWNTs-TiO_2/Ag and MWNTs-TiO_2/Ag conjugates exhibited significant inhibitory effects on these bacterial strains after 24 h of incubation. Furthermore, the cytotoxicity of these conjugates was assessed against uterine cancer (SiHa) and normal (WRL68) cell lines, revealing selective cytotoxicity towards tumor cells (~60% to 40%) while minimally impacting normal cells (~10%) (Fig. 5(d)).

Zhao *et al.* investigated the microstructural, mechanical, anticorrosive, and antibacterial characteristics of Mg–2.5Zn–0.5Zr/xCNT (x = 0, 0.3, 0.6, 0.9) composites.[80] In MTT assay, MG63 cells incubated in the nanocomposites for 3 and 7 days resulted in the number of viable cells being proportional to the amount absorbed (Fig. 5(e)). In particular, the number of viable cells in the nanocomposites gradually increased with the duration of incubation, but the increase in CNT content may lead to destruction by galvanic corrosion and increased toxicity.[81] These composites were meticulously fabricated through mechanical alloying and semi-powder metallurgy (SPM) processes, culminating in spark plasma sintering (SPS). Microstructural analysis demonstrated a nearly uniform distribution of CNTs within the Mg matrix. The findings highlighted significant enhancements in the hardness and ultimate compressive strength (UCS) of the composites compared to a pure Mg matrix. Additionally, introducing small amounts of CNTs led to an approximate 50% reduction in the degradation rate of the Mg composites when immersed in Kokubo-simulated body fluid (SBF). The antibacterial evaluation also demonstrated a preventive effect against the growth of *E. coli* and *S. aureus* with the inclusion of CNTs in the Mg matrix. These results endorse the potential of CNTs as an effective reinforcement for Mg–2.5Zn–0.5Zr/CNTs biocomposites, leading to notable improvements in mechanical, degradation, and antibacterial performance.

The unique characteristics CNTs make them advantageous for enhancing metal-based nanocomposites in biomedical applications. Their integration not only improves mechanical and electrical properties but also confers significant biocompatibility benefits. This synergy capitalizes on the mechanical robustness of metals combined with the unique attributes of CNTs, facilitating the tailoring of biocompatible properties in metal-based nanocomposites. Consequently, these materials demonstrate superior mechanical strength, meeting specific requirements of biomedical applications. The seamless fusion of CNTs and metals provides versatile solutions for medical devices, implants, and components, catering to diverse biocompatibility needs.

2.4. CNFs and their metal composites

Carbon nanofibers (CNFs) are a form of carbon nanomaterial characterized by their high aspect ratio and unique structure, where carbon atoms are arranged in a graphitic layered configuration, forming cylindrical shapes. This arrangement results in sp^2 hybridization, which provides CNFs with exceptional mechanical strength and electrical conductivity.[39,82,83] The structural integrity and versatility of CNFs make them highly applicable in various biomedical fields, such as scaffolds for tissue engineering due to their large specific surface area and porosity and biocompatibility.[84,85] Additionally, their capacity for ease functionalization with various chemical groups enhances their interaction with biological molecules. These properties can be used to create highly sensitive and selective sensors for the detection of biomolecules, which is crucial for the early diagnosis and monitoring of diseases. In particular, CNFs can be coated with biocompatible polymers to improve their dispersibility in biological fluids, making them effective carriers for targeted drug delivery.[86]

Jeong *et al.* proposed the use of Au NPs-loaded CNF (Au–S–CNF) as functional additives that are capable of reinforcing polycaprolactone (PCL) cardiovascular scaffolds and facilitating controlled drug delivery.[87] The study demonstrates that the inclusion of 0.5 wt% of Au–S–CNF, uniformly dispersed within the PCL matrix, significantly improves the scaffold's mechani-

cal properties, with an elastic modulus of 169 MPa and toughness of 334 J cm^{-3}, compared to bare PCL scaffolds. The application of these reinforced PCL composites in the fabrication of patient-specific cardiovascular drug-eluting scaffolds (CDECS) using a three-dimensional (3D) printing technique, as illustrated in Fig. 6(a). The fabricated cardiovascular scaffolds based on bare and 0.5 wt% functional additive reinforced PCL showed that the struts had a well-faceted and uniform shape and size (Fig. 6(b)). The feasibility of the proposed CDECS is validated through real-time X-ray imaging, which confirms the scaffold's visibility in a mouse thoracic cavity (Fig. 6(c)).

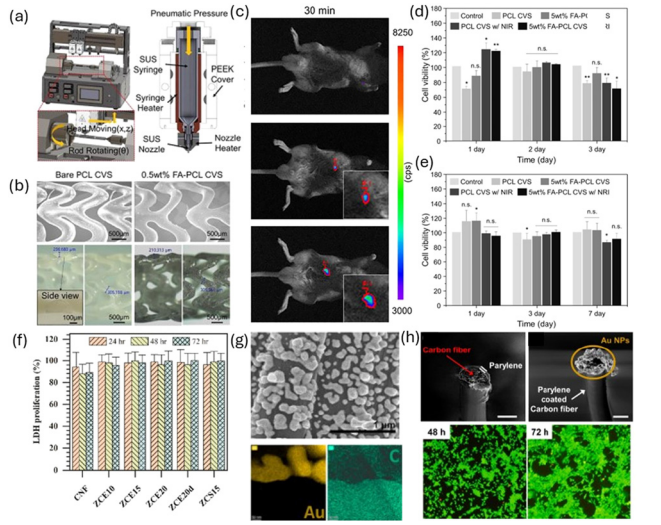

Fig. 6 (a) Prototype model of the custom-made 3D printing machine that has been used for the fabrication of functional additives reinforced PCL scaffold; (b) FESEM images of the bare and 0.5 wt% functional additives reinforced cardiovascular scaffolds, and optical images of the bare and 0.5 wt% functional additives reinforced PCL cardiovascular scaffold strut thickness and width. Inset shows the cross-sectional view of the strut thickness and width; (c) fluorescent images of the proposed cardiovascular scaffold at 30 min time points after the administration of DOX-coated functional additives reinforced scaffold and NIR irradiation (NIR: 808 nm wavelength and power of 3 W cm^{-2} for 10 min) and their quantitative plots of change of area and photon flux. FA and CVS in figures represents functional additives and cardiovascular scaffold, respectively; cytotoxicity analysis of the fabricated bare and functional additives reinforced cardiovascular scaffolds. Relative cell viability of human umbilical vein endothelial cells (HUVECs) (d) vascular smooth muscle cells (VSMCs) (e) after 1, 3, 7 day incubation with the bare and 0.5 wt% functional additives reinforced PCL cardiovascular scaffold with and without NIR irradiation, respectively. n = 4 (for each cell type). Reproduced with permission from ref. 87 Copyright © 2023 Elsevier. (f) Cell proliferation by LDH proliferation assay. Reproduced with permission from ref. 88 Copyright © 2023 Elsevier. (g) Au NP decoration by electrochemical deposition; SEM image of Au NP decoration on the CF surface and magnified Au NP images (HADDF) on the CF surface with EDS analysis; (h) DA detection for electrochemical biosensors; SEM images of CF encapsulated by biocompatible PEBAX and Au NP deposition on the exposed CF cross-section. Scale bar: 10 μm. Immunofluorescent images of 3T3 cultured around the CF/Au NP hybrid structure in the same well (green: live, red: dead cells); after 48 h (left) and 72 h (right). Reproduced with permission from ref. 89 Copyright © 2022 ACS.

Moreover, the study illustrates the dual functionality of these scaffolds, which can be used as both a standard drug-eluting cardiovascular scaffold (DECS) and an on-demand CDECS, activated by a near-infrared (NIR) light source (Fig. 6(d and e)).

Nekounam *et al.* studied the effects of ZnO NPs on various structural and non-structural properties of CNF meshes.[88] The study found that higher concentrations of ZnO NPs reduced conductivity but improved surface wettability by approximately 19–33%. Additionally, both direct and indirect cytotoxicity assays confirmed the excellent biocompatibility of the ZnO NP–CNF composites. MG-63 cells showed strong attachment and spreading across the surfaces of all tested nanocomposites (Fig. 6(f)).

Lim *et al.* developed a hybrid Au NPs-loaded lyocell-based carbon fiber composite (LCF/Au NP).[89] The LCF exhibited impressive mechanical properties with a tensile strength of 3 GPa and a Young's modulus of 28 GPa. Au NPs were electrochemically deposited onto the LCF surface from a biocompatible aqueous solution, significantly reducing impedance and increasing capacitive density due to the enhanced surface area. The deposition process confined nanoscale cracks to the surface of the LCFs, which did not adversely affect their mechanical properties (Fig. 6(g)). The biocompatibility of the LCF/Au NP hybrid was confirmed, highlighting its potential for electrochemical biosensors. Specifically, the researchers fabricated a carbon fiber-based dopamine (DA) monitoring tool, where Au NPs on the LCF surface enhanced electrochemical performance (Fig. 6(f)). This structure successfully detected DA with high sensitivity (0.320 μA μM^{-1}) and a limit of detection (LOD) of 25 nM. Additionally, the structure demonstrated appropriate selectivity under brain fluid conditions.

Overall, the synergistic effect of CNFs and their metal composites combines the mechanical robustness of metals with the unique properties of CNFs, allowing for tailored biocompatibility in metal-based nanocomposites. These hybrid materials exhibit superior mechanical strength and flexibility, meeting specific requirements for various biomedical applications. The high surface area and porosity of CNFs promote cell attachment and growth, making them ideal for tissue engineering scaffolds. Additionally, the excellent electrical conductivity of CNFs enhances the performance of biosensors, enabling more sensitive and accurate detection of biomolecules, which is critical for early disease diagnosis and monitoring. The functionalization can be used to develop drug delivery systems that efficiently target specific cells or tissues, thereby reducing side effects and improving therapeutic outcomes.

2.5. Graphene and their metal composites

Metal composites play a pivotal role as critical elements in biomedical applications, going beyond mere structural support. Their inherent properties, including biocompatibility and durability, can be precisely tailored to meet specific requirements. Titanium (Ti) and hydroxyapatite (HAP) are widely used in this field, with Ti being a preferred choice for medical

implants due to its excellent strength, corrosion resistance and natural bone bonding ability. A biocompatible ceramic, HAP effectively mimics the mineral component of bone. Composites of Ti and HAP are widely used in orthopedic implants, such as hip and knee replacements, to improve the long-term stability and integration of the implant into the human body. In addition, graphene, recognized for its biocompatibility, is emerging as an important reinforcing material in metal matrix composites. These composites, especially those reinforced with graphene, are essential to improving the durability and integration of implants in orthopedic applications.[90,91]

Graphene, a nanomaterial obtained by isolating a single layer of graphite, is central to both fundamental and applied research. The ideal graphene has a C–C bond length of ~0.14 nm and a thickness of ~0.35 nm. Its structure consists of hexagonally arranged carbon atoms forming a honeycomb lattice with π electron clouds and sp^2 hybridization.[92–94] The importance of graphene stems from its high surface area, exceptional electrical and thermal conductivity, and superior chemical and mechanical properties. This versatility extends to various forms, including pure graphene, graphene quantum dot (GQD), graphene oxide, and reduced graphene oxide, each of which offers unique advantages based on tunable surface chemistry and morphology.[95–99] In particular, GQDs, with their sub-30 nm size and functional groups such as hydrogen and oxygen, are utilized in free radical scavenging, biomedical imaging, drug delivery, and photoelectric applications.[100–102] In biomedical sensors, graphene is an integral part of field-effect transistors (FETs) for chemical and biological sensing.105–108 Graphene oxide is also used in gene therapy and delivery, protecting vectors and DNA during transport.[103–106] Also, graphene coatings on biomedical implants improve surface properties, mechanical strength, durability, and biocompatibility.

Munir *et al.* developed Mg metal matrix composites (MMCs) reinforced with graphene nanoplatelets (GNPs) using a powder metallurgy (PM) approach. This study involved dispersing GNPs in different concentrations (0.1, 0.2, and 0.3 wt%), layer thicknesses (5 nm and 9 nm), and particle sizes (15 μm and 5 μm) into Mg powder using high-energy ball milling processes.[107] They evaluated corrosion resistance through electrochemical tests and hydrogen evolution measurements and conducted cytotoxicity studies using osteoblast-like $SaOS_2$ cells. The research highlighted the effectiveness of GNPs as reinforcements in Mg matrices, particularly for the fabrication of biodegradable Mg-based composite implants. The incorporation of GNPs improved the mechanical properties of Mg through synergistic strengthening mechanisms. In addition, maintaining the structural integrity of GNPs during the manufacturing process improved the ductility, compressive strength, and corrosion resistance of the composites. Importantly, cytotoxicity evaluations indicated no significant toxicity from GNPs in Mg matrices.

Sharma *et al.* fabricated AZ31 (an alloy containing 3 wt% Al and 1 wt% Zn) reinforced with various weight percentages of graphene nanoplatelets (GNPs).[108] The reinforcement with 0.5, 1.5 and 3 wt% GNPs was carried out by powder metallurgy (PM) followed by sintering and hot extrusion. The objective of this study was to evaluate the effect of GNP content on the mechanical properties, microstructure, and wear resistance of AZ31 with a particular focus on biomedical applications. In particular, a significant increase in porosity was observed at 3 wt% GNP, indicating agglomeration and dispersion of GNPs within the metal matrix composite (MMC). Among the three samples, the lowest elongation was observed at 3 wt% GNP, indicating improved mechanical properties of the MMC. The research also revealed that toxicity increased with higher levels of GNP in AZ31. This research provided insight into the biomedical potential of the material through a series of tests, including tensile, microhardness, compression and wear tests.

Shahin *et al.* synthesized magnesium-based nanocomposites (MNCs) with matrices of $Mg_{0.5}Zr$ and $Mg_{0.5}Zr_xZn$ (x = 1–5 wt%) reinforced with various concentrations (0.1–0.5 wt%) of GNPs.[109] Employing PM, they thoroughly assessed the nanocomposites' mechanical and corrosion characteristics. Their findings revealed trends linked to GNP concentration in $Mg_{0.5}Zr$ matrices. Specifically, increasing GNP content from 0.2 wt% to 0.5 wt% in $Mg_{0.5}Zr$ matrices decreased compressive yield strength and corrosion resistance in Hanks' balanced salt solution (HBSS). Conversely, adding 4–5 wt% Zn to $Mg_{0.5}Zr_{0.1}$GNP improved ductility but reduced compressive yield strength. The optimal results were achieved with 0.1 wt% GNPs in $Mg_{0.5}Zr_3Zn$ matrices, exhibiting compressive strength (387 MPa) and yield strength (219 MPa). Notably, $Mg_{0.5}Zr_1Zn_{0.1}$GNP and $Mg_{0.5}Zr_3Zn_{0.1}$GNP nanocomposites showed experimental yield strengths approximately 29% and 34% higher, respectively, than the theoretical yield strength of $Mg_{0.5}Zr_{0.1}$GNP, attributable to synergistic strengthening mechanisms, including differences in thermal expansion, elastic modulus, particle geometry, grain refinement, load transfer, and the precipitation of GNPs within the Mg matrices. They also investigated corrosion rates in $Mg_{0.5}Zr_1Zn_{0.1}$GNP, $Mg_{0.5}Zr_3Zn_{0.1}$GNP, $Mg_{0.5}Zr_4Zn_{0.1}$GNP, and $Mg_{0.5}Zr_5Zn_{0.1}$GNP, using potential dynamic polarization, with rates ranging from 4.1 mm per year to 8.0 mm year. These results highlight the potential of GNPs in enhancing both mechanical properties and corrosion resistance of Mg–Zr–Zn matrices for biomedical applications.

The incorporation of graphene coatings into metal composites for biomedical applications represents a promising avenue for advancing the field. The synergistic combination of graphene's unique properties with the mechanical strength of metals offers comprehensive improvements in surface properties, mechanical robustness, durability, and biocompatibility for biomedical implants. This amalgamation holds significant potential for developing next-generation medical devices, implants, and components capable of addressing various challenges and requirements in the biomedical field.

2.6 DLC and their metal composites

DLC has gained widespread recognition across various academic and industrial sectors due to its exceptional stability, inert nature, and superior tribological and mechanical properties. Its inherent hardness and wear resistance make DLC

an ideal choice for dental and orthopedic implants.[110–112] Additionally, its excellent biocompatibility renders it invaluable in biomedical applications. Structural analysis indicates that DLC possesses an amorphous structure characterized by varying ratios of sp^2 and sp^3 bonded carbon atoms, often incorporating hydrogen.[113,114] The amorphous matrix predominantly features sp^3 nodules within an sp^2-bonded matrix. In contrast, graphite exhibits predominantly sp^2 bonding in a planar configuration, where each carbon atom forms a double bond and two single bonds, mostly with other carbon atoms. sp^3 bonded carbon atoms adopt a tetrahedral arrangement, forming three single bonds. The diverse combinations of carbon bonding types endow DLC coatings with unique properties, the application of which depends on the concentration and arrangement of these elements.[115–117] The intermediate properties of DLC, lying between diamond and graphite, include higher hardness, lower friction coefficient, exceptional tribological properties, and reduced wear rate.[118–120] The role of DLC in biomedicine is particularly important, offering hemocompatibility, anticancer potential, antithrombogenic properties, and antibacterial effects.

DLC coatings on metal composites have achieved significant recognition for enhancing the mechanical, tribological, electrical, optical, and biomedical characteristics of materials in biomedical engineering.[112,121,122] Their application in the medical sector is particularly noteworthy due to their combination of high hardness, low friction coefficient, minimal wear rates, and proven biocompatibility.[123–125] Thus, DLC coatings present a compelling option for various artificial implants, including hip and knee joints, bone plates, heart valves, heart diaphragms, stents, and splints.[126–129]

However, pure DLC coatings lack inherent *in vivo* anti-inflammatory properties. To overcome this limitation, they are often augmented with elements like silver (Ag), Titanium (Ti) tungsten (W), copper (Cu), platinum (Pt), zinc (Zn), and other metal ions, recognized for their biocompatibility, genotoxicity, antimicrobial properties, hemocompatibility, and ability to inhibit bacterial and tumor growth.[130–132] However, excessive metal content has been found to be cytotoxic to human cells, making systematic cytotoxic profiling of metal/DLC composites an important area of research.

Zhang *et al.* conducted a study on a series of Ti/Ti-DLC films carefully deposited onto monocrystalline Si substrates through a dual-magnetron sputtering process (Fig. 7(a–d)).[133] The research aimed to investigate the influence of Ti content on the properties of these films and their suitability for various medical applications. They observed that when the Ti content reached 4.43 atom%, the introduction of Ti into the DLC matrix triggered the formation of a TiC phase. This transition was accompanied by a gradual increase in surface roughness as the Ti content increased. Remarkably, Ti-DLC films containing 17.13 atom% Ti exhibited significant improvements in adhesion strength and surface hardness, indicating enhanced mechanical properties. Importantly, the study revealed that the optical densities (ODs) of the various Ti-DLC films remained comparable, indicating that these films retained biocompatibility regardless of their Ti content. This pivotal finding underscores the promise of Ti-doped DLC films for medical applications, as they offer a favorable balance of enhanced mechanical properties, as indicated by the elastic modulus, hardness, adhesion strength, and surface roughness while maintaining the essential attribute of biocompatibility.

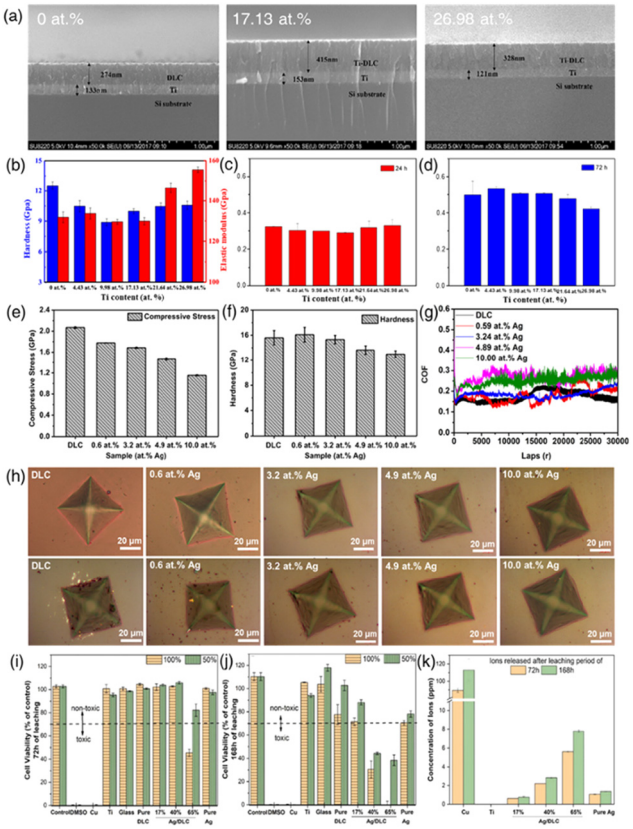

Fig. 7 (a) Cross-sectional SEM morphologies of Ti/Ti-DLC films prepared with varying Ti contents; (b) hardness and elastic modulus of Ti-DLC films as a function of Ti content; (c and d) cell proliferation on Ti-DLC films with different Ti contents. The data represent mean values with SD indicated. The "*" above the bar indicates statistical significance compared to the control group ($P < 0.05$). Reproduced with permission from ref. 133 Copyright © 2020 ACS. (e and f) Stress and hardness of the DLC film and Ag-DLC films with different Ag concentrations; (g) friction coefficients of the DLC film and Ag-DLC films with various Ag concentrations; (h) indentation morphologies of the DLC and Ag-DLC films as-deposited and after 300 days of immersion in PBS. Reproduced with permission from ref. 134 Copyright © 2021 Elsevier. (i and j) Biocompatibility of pure DLC, pure Ag, and Ag/DLC extracts obtained following 72 h and 168 h of leaching in undiluted (100%) DMEM and 50% diluted DMEM culture media, assessed on L929 mouse fibroblasts after 72 h of incubation, and (k) corresponding ion release concentrations measured with ICP-OES. Negative controls included Blank DMEM, Ti, and Glass extracts, while positive controls included Cu extracts and 10% DMSO. Reproduced with permission from ref. 112 Copyright © 2023 Elsevier.

Jing *et al.* prepared silver (Ag)-doped diamond-like carbon (Ag-DLC) films using a hybrid deposition technique that combined high-power pulsed magnetron sputtering (HPPMS) and high-power pulsed plasma-enhanced chemical vapor depo-

sition (HPP-PECVD) (Fig. 7(e–h)).[134] These films were deposited on Si wafer and Co–Cr–Mo alloy substrates, with Ag concentrations varying from 0.0 to 10.0 at%. Control of the Ag concentration was achieved by adjusting the number of Ag rods in the silver-graphite target mosaic. The study involved a comprehensive analysis of the impact of Ag doping on the microstructure, chemical bonding, mechanical properties, and adhesion stability of the DLC films. Notable findings indicated that Ag doping refined the columnar structure within the DLC films, leading to changes in the shape and size of DLC surface hillocks. With increasing Ag concentration, the residual stress within the DLC films diminished, enhancing the adhesion to the substrates. A significant outcome was that the proportion of sp^3 bonds in the carbon structure decreased as Ag concentration increased, resulting in reduced film hardness when Ag exceeded 3.2 at%. However, Ag doping improved the wear performance of DLC films, with the 3.2 at% Ag-DLC film demonstrating exceptional wear resistance. Additionally, Ag-DLC films exhibited superior adhesion stability in physiological solutions compared to pure DLC films, a crucial factor for their long-term performance in *in vivo* applications.

Zia *et al.* investigated Ag-enriched diamond-like carbon (Ag/DLC) coatings for medical applications. The introduction of Ag has been pivotal in enhancing the biocompatibility and antimicrobial properties of DLC, with higher Ag concentrations also improving hemocompatibility and inhibiting tumor growth (Fig. 7(i–k)).[112] Their study employed a novel co-sputter deposition to create Ag-enriched DLC coatings with Ag content levels of 17, 40, and 65 at%. A key aspect of their research was assessing the biocompatibility of Ag/DLC coatings, involving analysis of Ag ion release rates in Dulbecco's modified Eagle's medium over 72 and 168 h. The study utilized inductively coupled plasma optical emission spectroscopy and correlated the findings with biocompatibility profiles using the L929 mouse fibroblast cell line. Electron Dispersive X-ray (EDX) mapping revealed a uniform distribution of Ag within the DLC matrix. XRD diffraction patterns showed amorphous-like behavior for the 17 at% Ag/DLC coating, while the 40 and 65 at% Ag/DLC coatings displayed notable Ag crystallinity. A critical observation was that the 65 at% Ag/DLC coating, with a leached Ag ion concentration of 8 ppm, compromised biocompatibility. In contrast, the 17 at% Ag-enriched DLC coatings are deemed safe for biomedical applications and remained biocompatible even after prolonged ion leaching periods of 168 h and exhibited less significant mechanical property degradation compared to the 40 and 65 at% Ag/DLC coatings, which saw a decline of over 50%.

3. Figure-of-the merit of carbon materials and their metal composites for biomedical applications

Hybrid carbon/metal composites have garnered significant attention in the biomedical field due to their combined properties, which address the limitations of single-material systems. The integration of carbon materials with metals results in composites that are not only mechanically robust but also electrically conductive and biocompatible.

The figure-of-merit (FOM) is crucial for selecting materials to create hybrid carbon/metal composites for biomedical applications. It provides a comprehensive evaluation of key properties including mechanical strength, electrical conductivity, biocompatibility, functionalization potential, antimicrobial properties, and thermal conductivity. This assessment ensures the chosen materials meet specific application requirements, optimizing performance and safety. By highlighting the strengths and weaknesses of each material, the FOM plays a vital role in designing hybrid composites that leverage the synergistic benefits of both carbon and metal components, enhancing their performance and safety in specific demands of biomedical applications.

Table 1 summarizes the FOM for various carbon and metal materials in biomedical applications, highlighting key properties such as mechanical strength, electrical conductivity, biocompatibility, functionalization potential, antimicrobial properties, and thermal conductivity. These properties are critical for evaluating material performance in applications like biosensors, neural interfaces, and implants, and for enhancing interactions with biological systems while preventing infections. For carbon materials, fullerene offers unique antioxidant properties and potential for drug delivery, while CQDs stand out for their fluorescent properties and ease of functionalization, making them ideal for imaging and biosensing applications. CNTs are known for their exceptional mechanical strength and electrical conductivity, making them perfect for reinforcing metal matrices. Their high surface area and ability to be functionalized with bioactive molecules enhance their suitability for biomedical applications. CNFs offer high mechanical robustness and porosity, promoting cell attachment and growth, which is particularly beneficial for tissue engineering scaffolds. Graphene's superior mechanical, thermal, and electrical properties, combined with its large surface area, make it an excellent candidate for various biomedical applications, including drug delivery and biosensing. DLC, a 3D carbon material, provides high hardness and wear resistance, enhancing the durability of implants and devices. Its moderate biocompatibility and potential for surface functionalization make it suitable for a range of biomedical applications. Regarding metals, Au NPs are highly biocompatible and stable, with strong antimicrobial properties, and are easily functionalized, making them suitable for a wide range of biomedical applications. Ag NPs also possess excellent antimicrobial properties, crucial for preventing infections in medical devices and implants; however, their cytotoxicity at high concentrations requires careful control of their release rates. Ti and TIO_2 are renowned for their mechanical strength, corrosion resistance, and biocompatibility, ideal for orthopedic and dental implants, especially when integrated with carbon materials for enhanced properties. Zn is notable for its biodegradability and essential role in wound healing. Its high

Table 1 Summary of the figure-of-merit for various carbon and metal materials in biomedical applications, focusing on key properties including biocompatibility

Material	Mechanical strength	Electrical conductivity	Bio-compatibility	Functionalization potential	Antimicrobial properties	Thermal conductivity	Other notable properties
Fullerene	Moderate (6)	Moderate (6)	High (8)	High (8)	Moderate (6)	Moderate (6)	Antioxidant properties, potential drug delivery
CQDs	Moderate (5)	High (7)	Excellent (9)	High (9)	High (7)	Moderate (5)	Fluorescent properties, ease of functionalization
CNTs	Excellent (10)	Excellent (9)	High (8)	High (9)	Moderate (5)	High (7)	High surface area, flexibility
CNFs	High (8)	High (8)	High (7)	High (8)	Moderate (4)	Moderate (6)	Porosity, promotes cell growth
Graphene	High (7)	Excellent (9)	High (8)	High (8)	Moderate (5)	Excellent (10)	Large surface area, flexibility, thermal stability
DLC	High (8)	Moderate (5)	High (8)	Moderate (7)	Moderate (6)	High (8)	High hardness, wear resistance
Gold (Au) nanoparticles	Moderate (5)	High (7)	Excellent (9)	High (9)	High (9)	Low (4)	Stability, ease of functionalization
Silver (Ag) nanoparticles	Moderate (5)	Moderate (6)	High (7)	High (8)	Excellent (10)	Low (4)	Strong antimicrobial properties
Titanium (Ti)/titanium dioxide (TiO_2)	Excellent (9)	Moderate (5)	High (8)	Moderate (7)	Moderate (6)	Moderate (5)	Corrosion resistance, stability
Zinc (Zn)	High (6)	Moderate (6)	High (8)	High (8)	Excellent (9)	Moderate (6)	Biodegradable, essential for wound healing
Hybrid composites (carbon-metal)	Superior (10)	High (9)	Excellent (9)	High (10)	High (9)	High (8)	Synergistic properties, enhanced multifunctionality

The numbers in parentheses indicate the degree of weakness (1) to strength (10).

antimicrobial properties and moderate mechanical strength make it suitable for temporary implants and devices benefiting from controlled degradation. Hybrid composites combine the advantageous properties of both carbon and metal materials, resulting in enhanced mechanical strength, biocompatibility, and multifunctionality. These composites can be tailored for specific applications, such as tissue engineering scaffolds, drug delivery systems, and biosensors, by selecting appropriate carbon and metal components based on their FOM. For instance, incorporating Au NPs into a carbon matrix like fullerene or CQDs leverages their ability to control drug release through pore structure and surface chemistry, along with their antimicrobial properties, while mitigating cytotoxicity *via* controlled release mechanisms—ideal for targeted therapy. Combining CNTs with metals such as Ti significantly enhances the composite's mechanical properties and biocompatibility, providing robust scaffolds that support cell growth and tissue regeneration, ensuring long-term performance and safety in medical implants. Integrating graphene with Au or Ag NPs improves both electrical and thermal conductivity, crucial for biosensors and neural interfaces, thus enhancing sensitivity and accuracy for early disease diagnosis and monitoring. Additionally, hybrid composites can be functionalized with bioactive molecules to improve cell adhesion and growth, essential for tissue engineering and drug delivery applications. The careful integration and functionalization of these materials are key to maximizing their potential in advancing biomedical technologies.

4. Summary and outlook

Carbon-based metal nanocomposites surpass traditional metallic biomaterials, offering integrated advantages such as improved mechanical performance, enhanced biocompatibility, and facile surface modification for biomedical applications. These properties can be tailored to specific requirements. These advancements are categorized based on the dimensions of carbon materials, including fullerene and their metal nanocomposites, CQDs and their metal nanocomposites, CNFs and their metal nanocomposites, CNTs and their metal nanocomposites, graphene and its metal nanocomposites, and DLC and its nanocomposites.

Among carbon-based materials, fullerenes are composed of carbon atoms arranged in a hollow spherical or tubular structure. Due to their high electron affinity and exceptional chemical stability, fullerenes have emerged as promising materials for a wide range of applications in nanotechnology and biomedical fields. In particular, fullerenes have shown potential in drug delivery systems and photodynamic therapy. The ability of fullerenes to cross cell membranes and localize to specific cellular compartments enables targeted drug delivery that enhances therapeutic efficacy while minimizing systemic toxicity. The incorporation of fullerenes with metals to form hybrid nanocomposites has demonstrated high conductivity and catalytic activity, making them suitable for biomedical

applications. However, fullerenes are inherently hydrophobic and have a highly stable structure, which presents challenges for biodegradation in biological systems. Therefore, extensive research is required to elucidate the degradation pathways and by-products of fullerenes *in vivo*, as well as their distribution and excretion in biological environments.

CQDs, due to their nanoscale dimensions, offer significant advantages, particularly their exceptional biocompatibility, which facilitates seamless integration into biological systems without adverse effects. The tunable optical properties of CQDs, including photoluminescence, electrochemiluminescence, and varied electrochemical behaviors, combined with the functionalities of metal nanoparticles, are extensively applied in detecting biomacromolecules such as DNA, RNA, proteins, and glucose. This synergy results in superior selectivity and sensitivity, creating a versatile platform for bioimaging and diagnostic applications.

Additionally, leveraging the substantial surface area and impressive mechanical strength of CNTs, CNT-metal nanocomposites markedly improve biocompatibility and cellular interactions. However, it is essential to recognize that certain CNT types may cause inflammation. Nonetheless, their versatile properties make them suitable for a wide range of biomedical devices, from imaging to tissue engineering. Moreover, the integration of CNTs' electrical conductivity with metal complexation opens new avenues for exploring highly sensitive biomolecule detection, paving the way for advanced biosensors and diagnostic tools in biomedicine.

Functionalized CNFs offer significant advantages in biocompatibility and cellular interactions due to their high surface area and exceptional mechanical strength. The electrical conductivity of CNFs integrated with metallic elements paves the way for highly sensitive biomolecule detection. In addition, numerous studies have demonstrated the ability of CNFs to enhance the efficacy and chemosensitization of anticancer drugs against various types of tumors while minimizing side effects. Although applications of CNFs in biomedical fields are still more limited compared to other carbon-based materials, there is an urgent need for further research and exploration to fully elucidate and exploit the potential benefits of CNFs.

Graphene-metal nanocomposites possess a unique set of advantages attributed to graphene's exceptionally high surface area, electrical conductivity, mechanical strength, and distinctive 2D structure, which promotes exceptional cellular activity. The surface chemistry of these nanocomposites can be precisely customized, enhancing their interaction with biological entities. This customizability is particularly beneficial in targeted drug delivery for therapeutic applications. Moreover, GO and its derivatives demonstrate biocompatibility in both *in vitro* and *in vivo* environments and possess antibacterial properties, making them valuable in fields like tissue engineering. In enhancing antibacterial activity, these nanocomposites are utilized in photothermal therapy, where their synergy with laser light significantly improves their efficacy against bacterial agents.

DLC-metal nanocomposites exhibit superior hardness and wear resistance, enhancing the durability and longevity of biomedical devices. These properties make them particularly suitable for a variety of applications such as implants, artificial joints, bone engineering, and scaffold reinforcement. Additionally, DLC-metal nanocomposites are invaluable as wear-resistant coatings for medical devices, including orthopedic and dental implants, ensuring their extended functionality and reliability in clinical settings.

Despite their advantages, researchers recognize the critical need for comprehensive, long-term stability studies to ensure the reliability and safety of carbon nanomaterials in biomedical applications. Although substantial research has been conducted, it is important to acknowledge that this field is still nascent, with many biocompatibility studies being short-term relative to the human lifespan. Therefore, it is crucial to address the toxicity and side effects of carbon-based metal nanocomposites by developing methods to modify functionalities. This necessitates conducting in-depth and extended studies focusing on biocompatibility and cellular-level toxicity, rather than solely on genetic interactions, to thoroughly assess the safety and potential risks associated with their biomedical use.

Carbon materials and their metal composites take advantage of synergistic effects between the two components to provide properties not achievable by either material alone. Firstly, the integration of metals with carbon materials significantly increases mechanical strength. Doping carbon materials with metals strengthens the interfacial bond, improving tensile strength and Young's modulus. As a result, these hybrid composites are ideal for load-bearing biomedical applications, such as bone scaffolds and dental implants, where mechanical robustness is critical. Secondly, the electrical conductivity of carbon materials can be significantly improved through metal integration. The use of relatively non-toxic conductive metals provides conductive pathways at the carbon-metal interface, enhancing electrical properties. Improved electrical conductivity ensures fast and precise signal transmission, enhancing the performance and sensitivity of biomedical devices such as biosensors and neural interfaces. Finally, the antimicrobial properties of metal components combined with carbon materials open new avenues for infection prevention in biomedical applications. Integrating carbon materials with metal nanoparticles, recognized for their potent antimicrobial effects, results in composites that effectively disrupt bacterial cell membranes and inhibit microbial DNA replication. This provides a robust defense against infection. In addition, these hybrid composites retain and even enhance the inherent benefits of carbon materials, such as high surface area, mechanical strength, and biocompatibility.

In summary, this review highlighted significant advancements in the use of carbon nanomaterials in biomedicine, particularly in integrating metal nanoparticles and developing hybrid composites for various applications. The synergistic interaction between the unique properties of carbon nanomaterials and metals positions them as vital tools at the fore-

front of biomedical applications. This combination extends its influence across multiple domains, including diagnostics, imaging, drug delivery, and tissue engineering. As detailed in this article, the integration of carbon nanomaterials and metals heralds a promising era in biomedical research, spurring innovation and expanding possibilities for healthcare technologies.

Author contributions

Writing – original draft preparation S.-B. K., C.-H. K., S.-Y. L.; writing – review and editing, S.-B. K., C.-H. K., S.-Y. L., S.-J. P; supervision, S.-Y. L., S.-J. P. All the authors discussed and commented on the manuscript.

Data availability

No primary research results, software or code have been included and no new data were generated or analysed as part of this review.

Conflicts of interest

There are no conflicts to declare.

Acknowledgements

This research was supported by the National Research Foundation of Korea (NRF) grant funded by the Korea government (MSIT) (No. 2022M3J7A1062940). This work was supported by the National Research Foundation of Korea (NRF) grant funded by the Korea government (MSIT) (No. 2023R1A2C1004109). This work was supported by the Technology Innovation Program (or Industrial Strategic Technology Development Program- Development of technology on materials and components) (20010106, Adhesives with low water permeability and low outgassing) funded By the Ministry of Trade, Industry & Energy (MOTIE, Korea).

References

1 D. G. Anderson, J. A. Burdick and R. Langer, *Science*, 2004, **305**, 1923–1924.
2 N. A. Peppas and R. Langer, *Science*, 1994, **263**, 1715–1720.
3 J. Kohn, *Nat. Mater.*, 2004, **3**, 745–747.
4 M. Y. Liu, G. J. Zeng, K. Wang, Q. Wan, L. Tao, X. Y. Zhang and Y. Wei, *Nanoscale*, 2016, **8**, 16819–16840.
5 H. Y. Huang, R. M. Jiang, Y. L. Feng, H. Ouyang, N. G. Zhou, X. Y. Zhang and Y. Wei, *Nanoscale*, 2020, **12**, 1325–1338.
6 M. Pavlovic, A. Szerlauth, S. Muráth, G. Varga and I. Szilagyi, *Adv. Drug Delivery Rev.*, 2022, **191**, 114590.
7 A. Arsiwala, P. Desai and V. Patravale, *J. Controlled Release*, 2014, **189**, 25–45.
8 S. Abbaszadeh, V. Nosrati-Siahmazgi, K. Musaie, S. Rezaei, M. Qahremani, B. Xiao, H. A. Santos and M. A. Shahbazi, *Adv. Drug Delivery Rev.*, 2023, **200**, 115050.
9 L. Xiao, Y. P. Ma, R. Crawford, J. Mendhi, Y. Zhang, H. P. Lu, Q. Y. Zhao, J. Cao, C. T. Wu, X. Wang and Y. Xiao, *Mater. Today*, 2022, **54**, 202–224.
10 A. L. D. Santos, N. J. A. da Silva, C. T. R. Viana, L. C. C. dos Santos, G. H. C. da Silva, S. R. A. Scalzo, P. A. C. Costa, W. N. da Silva, I. C. G. de Jesus, A. Birbrair, M. T. Q. de Magalhaes, F. Frézard, S. Guatimosim, R. M. Haley, M. J. Mitchell, S. P. Andrade, P. P. Campos and P. P. G. Guimaraes, *Drug Delivery Transl. Res.*, 2023, **13**, 1420–1435.
11 Y. Y. Bao, N. Paunovic and J. C. Leroux, *Adv. Funct. Mater.*, 2022, **32**, 2109864.
12 J. Maughan, P. J. Gouveia, J. G. Gonzalez, L. M. Leahy, I. Woods, C. O'Connor, T. McGuire, J. R. Garcia, D. G. O'Shea, S. F. McComish, O. D. Kennedy, M. A. Caldwell, A. Dervan, J. N. Coleman and F. J. O'Brien, *Appl. Mater. Today*, 2022, **29**, 101629.
13 Q. S. Wang, X. Y. Yu, X. M. Chen, J. M. Gao, D. K. Shi, Y. Shen, J. Y. Tang, J. H. He, A. N. Li, L. Yu and J. D. Ding, *ACS Appl. Mater. Interfaces*, 2022, **14**, 24197–24212.
14 L. Ghasemi-Mobarakeh, D. Kolahreez, S. Ramakrishna and D. Williams, *Curr. Opin. Biomed. Eng.*, 2019, **10**, 45–50.
15 J. D. Bryers, C. M. Giachelli and B. D. Ratner, *Biotechnol. Bioeng.*, 2012, **109**, 1898–1911.
16 J. L. Hernandez and K. A. Woodrow, *Adv. Healthc. Mater.*, 2022, **11**, 2102087.
17 R. X. Wang, J. J. Sui and X. D. Wang, *ACS Nano*, 2022, **16**, 17708–17728.
18 S. T. Rajan, B. Subramanian and A. Arockiarajan, *Ceram. Int.*, 2022, **48**, 4377–4400.
19 S. Jhamb, J. Matai, J. Marwaha, A. Goyal and A. Pandey, *Adv. Mater. Processes Technol.*, 2023, **9**, 1249–1282.
20 S. Chen, R. Q. Zhao, X. Y. Sun, H. Z. Wang, L. Li and J. Liu, *Adv. Healthc. Mater.*, 2023, **12**, 2201924.
21 L. J. Mao, Y. R. Yin, L. X. Zhang, X. L. Chen, X. Q. Wang, F. P. Chen and C. S. Liu, *Adv. Healthc. Mater.*, 2022, **11**, 2101590.
22 C. A. Labarrere, A. E. Dabiri and G. S. Kassab, *Front. Bioeng. Biotechnol.*, 2020, **8**, 123.
23 G. Schmalz and K. M. Galler, *Dent. Mater.*, 2017, **33**, 382–393.
24 P. Joshi, R. Mishra and R. J. Narayan, *Curr. Opin. Biomed. Eng.*, 2021, **18**, 100274.
25 M. Islam, A. D. Lantada, D. Mager and J. G. Korvink, *Adv. Healthc. Mater.*, 2022, **11**, 2101834.
26 M. Mahmoudpour, J. E. N. Dolatabadi, M. Hasanzadeh and J. Soleymani, *Adv. Colloid Interface Sci.*, 2021, **298**, 102550.

27 X. Sun, J. C. Bao, K. Li, M. D. Argyle, G. Tan, H. Adidharma, K. H. Zhang, M. H. Fan and P. Ning, *Adv. Funct. Mater.*, 2021, **31**, 2006287.
28 X. H. Wang, H. R. Cheng, G. Z. Ye, J. Fan, F. Yao, Y. Q. Wang, Y. J. Jiao, W. F. Zhu, H. M. Huang and D. Q. Ye, *Chemosphere*, 2022, **287**, 131995.
29 C. H. Kim, S. Y. Lee and S. J. Park, *Green Chem.*, 2024, **26**, 1901–1909.
30 C. H. Kim, S. Y. Lee and S. J. Park, *J. CO2 Util.*, 2021, **54**, 101770.
31 G. Rajakumar, X. H. Zhang, T. Gomathi, S. F. Wang, M. A. Ansari, G. Mydhili, G. Nirmala, M. A. Alzohairy and I. M. Chung, *Processes*, 2020, **8**, 355.
32 M. Mohajeri, B. Behnam and A. Sahebkar, *J. Cell Physiol.*, 2019, **234**, 298–319.
33 R. Eivazzadeh-Keihan, A. Maleki, M. de la Guardia, M. S. Bani, K. K. Chenab, P. Pashazadeh-Panahi, B. Baradaran, A. Mokhtarzadeh and M. R. Hamblin, *J. Adv. Res.*, 2019, **18**, 185–201.
34 Z. L. Peng, T. S. Zhao, Y. Q. Zhou, S. H. Li, J. J. Li and R. M. Leblanc, *Adv. Healthc. Mater.*, 2020, **9**, 1901495.
35 Z. L. Peng, E. H. Miyanji, Y. Q. Zhou, J. Pardo, S. D. Hettiarachchi, S. H. Li, P. L. Blackwelder, I. Skromne and R. M. Leblanc, *Nanoscale*, 2017, **9**, 17533–17543.
36 N. Azam, M. N. Ali and T. J. Khan, *Front. Mater.*, 2021, **8**, 700403.
37 L. Bao, X. J. Cui, M. Mortimer, X. Y. Wang, J. G. Wu and C. Y. Chen, *Nano Today*, 2023, **49**, 101784.
38 A. Sobajima, T. Okihara, S. Moriyama, N. Nishimura, T. Osawa, K. Miyamae, H. Haniu, K. Aoki, M. Tanaka, Y. Usui, K. Sako, H. Kato and N. Saito, *ACS Biomater. Sci. Eng.*, 2020, **6**, 7032–7040.
39 G. G. Abdo, M. M. Zagho, A. E. Al Moustafa, A. Khalil and A. A. Elzatahry, *J. Biomed. Mater. Res., Part B*, 2021, **109**, 1893–1908.
40 R. Jain, H. G. Chae and S. Kumar, *Compos. Sci. Technol.*, 2013, **88**, 134–141.
41 S. Han, J. Sun, S. B. He, M. L. Tang and R. J. Chai, *Am. J. Transl. Res.*, 2019, **11**, 3246–3260.
42 K. S. Munir, C. Wen and Y. C. Li, *Adv. Biosyst.*, 2019, **3**, 1800212.
43 R. K. Roy and K. R. Lee, *J. Biomed. Mater. Res., Part B*, 2007, **83b**, 72–84.
44 A. W. Zia, I. Anestopoulos, M. I. Panayiotidis and M. Birkett, *Ceram. Int.*, 2023, **49**, 17203–17211.
45 P. Sarkar, K. Ghosal, D. Chakraborty and K. Sarkar, in *Handbook of Carbon-Based Nanomaterials*, Elsevier, 2021, pp. 829–875.
46 O. Erol, I. Uyan, M. Hatip, C. Yilmaz, A. B. Tekinay and M. O. Guler, *Nanomedicine*, 2018, **14**, 2433–2454.
47 L. Fritea, F. Banica, T. O. Costea, L. Moldovan, L. Dobjanschi, M. Muresan and S. Cavalu, *Materials*, 2021, **14**, 6319.
48 G. Redondo-Fernandez, J. C. Canga, A. Soldado, J. R. Encinar and J. M. Costa-Fernandez, *Anal. Chim. Acta*, 2023, 341874.
49 S. Grade, J. Eberhard, J. Jakobi, A. Winkel, M. Stiesch and S. Barcikowski, *Gold Bull.*, 2014, **47**, 83–93.
50 X. Jiang, B. Du, Y. Huang and J. Zheng, *Nano Today*, 2018, **21**, 106–125.
51 M. Chen, R. Guan and S. Yang, *Adv. Sci.*, 2019, **6**, 1800941.
52 H. Kazemzadeh and M. Mozafari, *Drug Discovery Today*, 2019, **24**, 898–905.
53 M. E. A. Ribeiro, N. R. C. Huaman, M. M. Folly, J. G. C. Gomez and R. J. S. Rodríguez, *Int. J. Biol. Macromol.*, 2023, **251**, 126531.
54 J. Shi, X. Yu, L. Wang, Y. Liu, J. Gao, J. Zhang, R. Ma, R. Liu and Z. Zhang, *Biomaterials*, 2013, **34**, 9666–9677.
55 M. R. Hamblin, *Photochem. Photobiol. Sci.*, 2018, **17**, 1515–1533.
56 P. Innocenzi and L. Stagi, *Chem. Sci.*, 2020, **11**, 6606–6622.
57 A. Kerna, K. Pruitt, J. Flores and U. Nwokorie, *EC Endocrinol. Metab. Res.*, 2020, **5**, 56–66.
58 N. M. Thong, Q. V. Vo, T. Le Huyen, M. Van Bay, N. N. Dung, P. T. T. Thao and P. C. Nam, *RSC Adv.*, 2020, **10**, 14595–14605.
59 M. J. Ansari, A. Soltani, M. Ramezanitaghartapeh, P. Singla, M. Aghaei, H. K. Fadafan, S. A. Khales, M. Shariati, H. Shirzad-Aski and H. Balakheyli, *J. Mol. Liq.*, 2022, **348**, 118083.
60 T. Anusha, K. S. Bhavani, J. S. Kumar and P. K. Brahman, *Diamond Relat. Mater.*, 2020, **104**, 107761.
61 T. Li and H. C. Dorn, *Small*, 2017, **13**, 1603152.
62 Y. Li, R. Biswas, W. P. Kopcha, T. Dubroca, L. Abella, Y. Sun, R. A. Crichton, C. Rathnam, L. Yang and Y. W. Yeh, *Angew. Chem.*, 2023, **135**, e202211704.
63 T. Li, L. Xiao, J. Yang, M. Ding, Z. Zhou, L. LaConte, L. Jin, H. C. Dorn and X. Li, *ACS Appl. Mater. Interfaces*, 2017, **9**, 17681–17687.
64 M. J. Molaei, *RSC Adv.*, 2019, **9**, 6460–6481.
65 A. Vibhute, T. Patil, R. Gambhir and A. P. Tiwari, *Appl. Surf. Sci. Adv.*, 2022, **11**, 100311.
66 H. L. Yang, L. F. Bai, Z. R. Geng, H. Chen, L. T. Xu, Y. C. Xie, D. J. Wang, H. W. Gu and X. M. Wang, *Mater. Today Adv.*, 2023, **18**, 100376.
67 X. Y. Xu, H. Min and Y. Li, *Anal. Methods*, 2023, **15**, 5731–5753.
68 S. Gurung, N. Arun, M. Joshi, T. Jaiswal, A. P. Pathak, P. Das, A. K. Singh, A. Tripathi and A. Tiwari, *Chemosphere*, 2023, **339**, 139638.
69 R. F. Nafchi, R. Ahmadi, M. Heydari, M. R. Rahimipour, M. J. Molaei and L. Unsworth, *Langmuir*, 2022, **38**, 3804–3816.
70 M. J. Molaei, *Sci. Rep.*, 2022, **12**, 17681.
71 T. Sarkar, T. K. Dhiman, R. K. Sajwan, S. Sri and P. R. Solanki, *Nanotechnology*, 2020, **31**, 355502.
72 M. S. Ardestani, Z. Zaheri, P. Mohammadzadeh, A. Bitarafan-Rajabi and S. M. Ghoreishi, *Bioorg. Chem.*, 2021, **115**, 105211.
73 S. Jin, O. Allam, K. Lee, J. Lim, M. J. Lee, S. H. Loh, S. S. Jang and S. W. Lee, *Small*, 2022, **18**, 2202898.
74 T. T. Qiang, S. T. Wang, L. F. Ren and X. D. Gao, *J. Environ. Chem. Eng.*, 2022, **10**, 108784.

75 J. A. Ferreira, L. C. Lieb, D. Y. Tiba, M. M. da Silva, A. C. Oliveira and T. C. Canevari, *Curr. Nanosci.*, 2024, **20**, 31–46.
76 F. Norouzi, M. Pourmadadi, F. Yazdian, K. Khoshmaram, J. Mohammadnejad, M. H. Sanati, F. Chogan, A. Rahdar and F. Baino, *J. Funct. Biomater.*, 2022, **13**, 300.
77 R. J. De, K. W. Jo, B. H. Lee, S. Some and K. T. Kim, *J. Mater. Chem. B*, 2023, **11**, 6024–6043.
78 S. Abazari, A. Shamsipur, H. R. Bakhsheshi-Rad, M. Keshavarz, M. Kehtari, S. Ramakrishna and F. Berto, *J. Mater. Res. Technol.*, 2022, **20**, 976–990.
79 D. S. Ahmed, M. K. A. Mohammed and M. R. Mohammad, *Chem. Pap.*, 2020, **74**, 197–208.
80 J. G. Zhao, H. W. Ma, A. Saberi, Z. Heydari and M. S. Baltatu, *Coatings*, 2022, **12**, 1589.
81 C. Shuai, S. Li, G. Wang, Y. Yang, S. Peng and C. Gao, *Mater. Sci. Eng., C*, 2019, **104**, 109935.
82 J. Gopinathan, M. M. Pillai, K. S. Sahanand, B. D. Rai, R. Selvakumar and A. Bhattacharyya, *Biomed. Mater.*, 2017, **12**, 065001.
83 Y. Tufan, H. Öztatlı, B. Garipcan and B. Ercan, *Biomed. Mater.*, 2021, **16**, 025027.
84 K. W. Chan, C. Z. Liao, H. M. Wong, K. W. K. Yeung and S. C. Tjong, *RSC Adv.*, 2016, **6**, 19417–19429.
85 D. Yadav, F. Amini and A. Ehrmann, *Eur. Polym. J.*, 2020, **138**, 109963.
86 D. A. Stout, *Curr. Pharm. Des.*, 2015, **21**, 2037–2044.
87 Y.-J. Jeong, S. Jeong, S. Kim, H. J. Kim, J. Jo, A. Shanmugasundaram, H. Kim, E. Choi and D.-W. Lee, *Chem. Eng. J.*, 2023, **454**, 140118.
88 H. Nekounam, S. Samani, H. Samadian, M. A. Shokrgozar and R. Faridi-Majidi, *Mater. Chem. Phys.*, 2023, **295**, 127052.
89 T. Lim, S. Won, I.-W. Nam, J. S. Choi, C. H. Kim, T. H. Kim, J. H. Kim, S. Y. Yeo, H. Zhang and B. J. Yeang, *ACS Sustainable Chem. Eng.*, 2022, **10**, 8815–8824.
90 W. S. Kang, K. Y. Rhee and S. J. Park, *Composites, Part B*, 2017, **114**, 175–183.
91 K. S. Kim and S. J. Park, *Electrochim. Acta*, 2011, **56**, 1629–1635.
92 N. M. El-Shafai, N. A. Alamrani, A. M. Al-bonayan, S. Abu-Melha, N. M. El-Metwaly and I. El-Mehasseb, *Surf. Interfaces*, 2023, **38**, 102757.
93 D. Deepak, N. Soin and S. S. Roy, *Mater. Today Commun.*, 2023, **34**, 105412.
94 X. Yang and B. Zhang, *Sci. Rep.*, 2023, **13**, 4364.
95 L. L. Huang, L. K. Ma, H. M. Chen, L. Qiao, L. T. Zhang, J. Pan, J. W. Li and Y. Z. Zhang, *J. Appl. Polym. Sci.*, 2023, **140**, e53507.
96 A. Joy, G. Unnikrishnan, M. Megha, M. Haris, J. Thomas, A. Deepti, P. S. B. Chakrapani, E. Kolanthai and S. Muthuswamy, *Diamond Relat. Mater.*, 2023, **136**, 110033.
97 S. W. Vedakumari, S. J. V. Jancy, Y. R. Pravin, J. Bhoopathy, K. Iyswariya, S. Thomas, R. Rubiya, L. Prabakaran, C. Kumar, P. Prabu and R. Murugesan, *Environ. Res.*, 2022, **209**, 112925.
98 L. Daneshmandi, M. Barajaa, A. T. Rad, S. A. Sydlik and C. T. Laurencin, *Adv. Healthc. Mater.*, 2021, **10**, 2001414.
99 L. Cao, F. Zhang, Q. G. Wang and X. F. Wu, *Mater. Sci. Eng., C*, 2017, **79**, 697–701.
100 A. M. Itoo, S. L. Vemula, M. T. Gupta, M. V. Giram, S. A. Kumar, B. Ghosh and S. Biswas, *J. Controlled Release*, 2022, **350**, 26–59.
101 A. M. L. Oliveira, M. Machado, G. A. Silva, D. B. Bitoque, J. T. Ferreira, L. A. Pinto and Q. Ferreira, *Nanomaterials*, 2022, **12**, 1149.
102 N. B. Moghadam, M. Avatefi, M. Karimi and M. Mahmoudifard, *J. Mater. Chem. B*, 2023, **11**, 2568–2613.
103 M. Azimzadeh, Z. Aghili, B. Jannat, S. Jafari, S. R. Tafti and N. Nasirizadeh, *IET Nanobiotechnol.*, 2022, **16**, 190–198.
104 M. M. Kadhim, A. M. Rheima, Z. S. Abbas, H. H. Jlood, S. K. Hachim, W. R. Kadhum and E. Kianfar, *RSC Adv.*, 2023, **13**, 2487–2500.
105 S. J. Heerema and C. Dekker, *Nat. Nanotechnol.*, 2016, **11**, 127–136.
106 D. B. Wells, M. Belkin, J. Comer and A. Aksimentiev, *Nano Lett.*, 2012, **12**, 4117–4123.
107 K. Munir, C. Wen and Y. C. Li, *J. Magnesium Alloys*, 2020, **8**, 269–290.
108 S. K. Sharma and K. K. Saxena, *Mater. Today: Proc.*, 2022, **56**, 2278–2287.
109 M. Shahin, C. E. Wen, K. Munir and Y. C. Li, *J. Magnesium Alloys*, 2022, **10**, 458–477.
110 B. Rothammer, K. Neusser, M. Bartz, S. Wartzack, A. Schubert and M. Marian, *Wear*, 2023, **523**, 204728.
111 C. C. Wachesk, S. H. Seabra, T. A. T. Dos Santos, V. J. Trava-Airoldi, A. O. Lobo and F. R. Marciano, *J. Mater. Sci.: Mater. Med.*, 2021, **32**, 117.
112 A. W. Zia, I. Anestopoulos, M. I. Panayiotidis, L. Bowen and M. Birkett, *J. Alloys Compd.*, 2023, **958**, 170473.
113 H. X. Sheng, W. W. Xiong, S. S. Zheng, C. Chen, S. He and Q. J. Cheng, *Carbon Lett.*, 2021, **31**, 929–939.
114 E. C. T. Ba, M. R. Dumont, P. S. Martins, B. D. Pinheiro, M. P. M. da Cruz and J. W. Barbosa, *Diamond Relat. Mater.*, 2022, **122**, 108818.
115 D. K. Rajak, A. Kumar, A. Behera and P. L. Menezes, *Appl. Sci.*, 2021, **11**, 4445.
116 J. Wei, H. C. Li, L. L. Liu, P. Guo, P. L. Ke and A. Y. Wang, *Surf. Coat. Technol.*, 2019, **374**, 317–326.
117 Y. F. Yu, X. Zhang, S. W. Yin, L. C. Bai and Z. S. Liu, *J. Non-Cryst. Solids*, 2022, **577**, 121318.
118 X. Y. Wang, X. Zhang, C. Wang, Y. Lu and J. Y. Hao, *Tribol. Int.*, 2022, **175**, 107845.
119 Y. Q. Shen, J. Luo, B. Liao, X. Zhang, Y. Y. Zhao, X. M. Zeng, L. Chen, P. Pang and F. Bao, *Diamond Relat. Mater.*, 2022, **125**, 108985.
120 M. Evaristo, F. Fernandes and A. Cavaleiro, *Wear*, 2023, **526**, 204880.
121 W. S. Li, Y. T. Zhao, D. Q. He, Q. Song, X. W. Sun, S. C. Wang, H. M. Zhai, W. W. Zheng and R. J. K. Wood, *Surf. Coat. Technol.*, 2022, **434**, 128198.

122 B. Z. Dong, X. H. Guo, K. D. Zhang, Y. P. Zhang, Z. H. Li, W. S. Wang and C. Cai, *Surf. Coat. Technol.*, 2022, **429**, 127951.
123 M. P. Nikolova and M. D. Apostolova, *Materials*, 2023, **16**, 183.
124 Y. Z. Bu, K. H. Yu, B. Zhang, B. Kuang and L. Qiang, *Coatings*, 2023, **13**, 320.
125 P. Joshi, P. R. Riley, W. Denning, S. Shukla, N. Khosla, J. Narayan and R. Narayan, *J. Mater. Chem. C*, 2022, **10**, 2965–2975.
126 M. Heitkemper, S. Sivakumar, H. Hatoum, J. Dollery, S. M. Lilly and L. P. Dasi, *J. Thorac. Cardiovasc. Surg.*, 2021, **162**, 1075–1083.
127 L. Gopal and T. Sudarshan, *Surf. Eng.*, 2023, **39**, 387–391.
128 C. Jongwannasiri, A. Krasaesin, S. Pinijsuwan, S. Udomsom, L. Boonprakong, K. Eawsakul, T. Osathanon and C. Manaspon, *Diamond Relat. Mater.*, 2023, **136**, 110022.
129 J. W. Shim, I. H. Bae, M. H. Jeong, D. S. Park, K. S. Lim, J. U. Kim, M. K. Kim, J. H. Kim, J. H. Kim and D. S. Sim, *Met. Mater. Int.*, 2020, **26**, 1455–1462.
130 N. Aslan, M. S. Kurt and M. M. Koç, *J. Electron. Mater.*, 2023, **52**, 2807–2818.
131 Y. F. Zhou, L. L. Li, W. Shao, Z. H. Chen, S. F. Wang, X. L. Xing and Q. X. Yang, *Diamond Relat. Mater.*, 2020, **107**, 107870.
132 C. L. Yan, P. Guo, J. Y. Zhou, R. D. Chen and A. Y. Wang, *Diamond Relat. Mater.*, 2023, **136**, 109935.
133 M. Q. Zhang, T. Y. Xie, X. Z. Qian, Y. Zhu and X. M. Liu, *ACS Omega*, 2020, **5**, 22772–22777.
134 P. P. Jing, D. L. Ma, Y. L. Gong, X. Y. Luo, Y. Zhang, Y. J. Weng and Y. X. Leng, *Surf. Coat. Technol.*, 2021, **405**, 126542.